Alexandria Engineering Journal (2020) 59, 2391–2400

HOSTED BY

ELSEVIER

Alexandria University

Alexandria Engineering Journal

www.elsevier.com/locate/aej
www.sciencedirect.com

ORIGINAL ARTICLE

Efficient sustainable algorithm for numerical solutions of systems of fractional order differential equations by Haar wavelet collocation method

Thabet Abdeljawad [a,f,g], Rohul Amin [b], Kamal Shah [c], Qasem Al-Mdallal [d,*], Fahd Jarad [e]

[a] *Department of Mathematics and General Sciences, Prince Sultan University, Riyadh, Saudi Arabia*
[b] *Department of Mathematics, University of Peshawar, Khyber Pakhtunkhwa, Pakistan*
[c] *Department of Mathematics, University of Malakand, Dir(L), Khyber Pakhtunkhwa, Pakistan*
[d] *Department of Mathematical Sciences, UAE University, P. O. Box 15551, Al Ain, United Arab Emirates*
[e] *Department of Mathematics, Çankaya University, 06790 Etimesgut, Ankara, Turkey*
[f] *Department of Medical Research, China Medical University, Taichung, Taiwan*
[g] *Department of Computer Science and Information Engineering, Asia University, Taichung, Taiwan*

Received 21 January 2020; revised 28 February 2020; accepted 29 February 2020
Available online 30 March 2020

KEYWORDS

Haar wavelet;
Collocation method;
Approximate solution;
Fractional differential equations

Abstract This manuscript deals a numerical technique based on Haar wavelet collocation which is developed for the approximate solution of some systems of linear and nonlinear fractional order differential equations (FODEs). Based on these techniques, we find the numerical solution to various systems of FODEs. We compare the obtain solution with the exact solution of the considered problems at integer orders. Also, we compute the maximum absolute error to demonstrate the efficiency and accuracy of the proposed method. For the illustration of our results we provide four test examples. The experimental rates of convergence for different number of collocation point is calculated which is approximately equal to 2. Fractional derivative is defined in the Caputo sense.

© 2020 The Authors. Published by Elsevier B.V. on behalf of Faculty of Engineering, Alexandria University. This is an open access article under the CC BY license (http://creativecommons.org/licenses/by/4.0/).

1. Introduction

Fractional Derivative (FD) is the generalization of ordinary derivative in which the order of the derivative is not an integer. The concept of FD was introduced by Riemann and Liouville. Due to its applications in various branches of science, fractional calculus attracted mathematicians in the last few decades [1,2]. In fact, the fractional calculus studies integrals and derivatives of any order. FODEs is the generalizations of integer order differential equations, which are used increasingly to model problems in physical, biological and other disciplines like engineering and technology [3–6]. This is because of the fact that fractional differential operator is a global operator and has greater degree of freedom. Further the aforesaid

* Corresponding author.
E-mail addresses: tabdeljawad@psu.edu.sa (T. Abdeljawad), raminmath@uop.edu.pk (R. Amin), q.almdallal@uaeu.ac.ae (Q. Al-Mdallal), fahd@cankaya.edu.tr (F. Jarad).

Peer review under responsibility of Faculty of Engineering, Alexandria University.

https://doi.org/10.1016/j.aej.2020.02.035
1110-0168 © 2020 The Authors. Published by Elsevier B.V. on behalf of Faculty of Engineering, Alexandria University.
This is an open access article under the CC BY license (http://creativecommons.org/licenses/by/4.0/).

operator has the ability to model real world phenomenon in more racialistic way as compared to integer order differential equations. Due to these significant devotion has been paid by the researchers to investigate FODEs from different aspects. The mentioned aspects are qualitative theory for existence of solutions, stability analysis and numerical analysis. As we know that the area devoted to establish existence theory for solutions to FODEs and their system has been very well established and a lot of papers are presented in literature in this regard [7–19]. On the other hand, to find the exact solution of FODEs are not available in general. Therefore strong motivation has been recorded in last two decades to establish some accurate numerical schemes. In this regard different schemes (methods) have been applied for integer order differential equations were further generalized to find the approximate solutions of FODEs and their systems. Here we remark that perturbation techniques, decompositions methods, power series methods and monotone iterative techniques have been applied very well so far for FODEs and their systems [20–31]. Besides from the aforesaid methods a variety of schemes have been generalized to find numerical solutions to FODEs. In recent time, the differential, integral and integro-differential equations have been solved by utilizing radial basis functions technique [32], the collocation and Tau method [33], Variational iteration method [34], the Legendre [35], Jacobi [36] and Bernstein operational matrices methods [37]. Arqub [38] found the numerical solution of fractional order systems. Arqub and Shawagfeh [39] developed algorithm for the solution of Dirichlet time-fractional diffusion-Gordon types equations in porous media. Arqub [40] used residual power series method for the solution of time-fractional Schrodinger equations in one-dimensional space. Arqub [41] explored the numerical solution of systems of first order, two-point BVPs based on the reproducing kernel algorithm. Also the wavelet methods have been given much attentions. The mentioned methods include Shifted Chebyshev technique [42], Sine–Cosine operational matrix [43], etc. Chen and Hsiao [44] in 1997 proposed for the first time the idea of Haar matrix for the integration of Haar functions and then applied it solve differential equations. This remarkable concept provided base for construction of general formalism of an operational matrix of integration for Haar wavelets. After this various wavelet methods have been developed by using orthogonal polynomials like the Legendre Wavelets operational matrix [35], the Chebyshev Wavelets methods [45], etc for the numerical solutions of FODEs. On the other hand HWCM has been used in large number for the approximate solutions to various classes of differential equations, see [46–48], etc. The concern method has many application, see [49]. Some of the recent work utilizing Haar wavelet collection method (HWCM) can be found in the references [50–53]. The HWCM has been increasingly used to solve FODEs [54–56]. The concerned scheme has mainly used for various classes of linear and nonlinear FODEs including scaler problems. Here we remark that we apply the proposed technique for solutions of coupled systems including nonlinear and linear FODEs.

The aforementioned differential operator is the generalization of ordinary derivative. Further we remark that fractional differential and integral operators have several definitions in which Caputo definition has been considered very well. Because the said derivative has been used for its convenient status. In this article we study a class of linear system of FODEs by considering Caputo's definition of the derivative given by.

$$\begin{cases} {}_0^C\mathrm{D}_t^{\alpha}\mathrm{x}(t) = \mathrm{ax}(t) + \mathrm{by}(t), & 0 < \alpha \leqslant 1, \\ {}_0^C\mathrm{D}_t^{\beta}\mathrm{y}(t) = \mathrm{cx}(t) + \mathrm{dy}(t), & 0 < \beta \leqslant 1, \end{cases} \tag{1}$$

with initial conditions:

$$\mathrm{x}(0) = \mathrm{x}_0 \text{ and } \mathrm{y}(0) = \mathrm{y}_0. \tag{2}$$

In same line we also investigate the given coupled system with Caputo's derivative of nonlinear FODEs as

$$\begin{cases} {}_0^C\mathrm{D}_t^{\alpha}\mathrm{x}(t) = \mathrm{ax}(t), & 0 < \alpha \leqslant 1, \\ {}_0^C\mathrm{D}_t^{\beta}\mathrm{y}(t) = \mathrm{bx}^2(t), & 0 < \beta \leqslant 1, \\ {}_0^C\mathrm{D}_t^{\gamma}\mathrm{z}(t) = \mathrm{cx}(t)\mathrm{y}(t), & 0 < \gamma \leqslant 1, \end{cases} \tag{3}$$

with initial conditions:

$$\mathrm{x}(0) = \mathrm{x}_0, \quad \mathrm{y}(0) = \mathrm{y}_0, \quad \mathrm{z}(0) = \mathrm{z}_0, \tag{4}$$

where ${}_0^C\mathrm{D}_t^{\alpha}, {}_0^C\mathrm{D}_t^{\beta}, {}_0^C\mathrm{D}_t^{\gamma}$ denotes the Caputo fractional derivatives of order α, β, γ respectively, a, b, c, d and $\mathrm{x}_0, \mathrm{y}_0, \mathrm{z}_0$ are any real constants in both considered problems.

The paper is organized in the following structure. Definition of HW is given in Section 2. Numerical technique for the solution of nonlinear and linear FDEs in view of the HWCM is developed in Section 3. In Section 4 some examples are given for validity and accuracy of our technique. Finally, conclusion is given in Section 5.

2. Some Axillary results and introduction to Haar wavelet

We split this section into two subsection as follows:

2.1. Axillary results about fractional calculus

In this subsection, we define some basic definitions:

Definition 2.1. Let $[0, b] \subset \mathrm{R}$, the Riemann–Liouville fractional order $\alpha \in \mathrm{R}_+$ of a function $\mathrm{u} \in (L[0, b], \mathrm{R})$ is given by [9,12]

$${}_0\mathrm{I}_t^{\alpha}\mathrm{u}(t) = \frac{1}{\Gamma(\alpha)} \int_0^t (t - \eta)^{\alpha - 1} \mathrm{u}(\eta) d\eta, \tag{5}$$

provided that the integral on the right hand side exists.

Definition 2.2. Let $\mathrm{u} : [0, \infty) \to \mathrm{R}$, be any function, then Caputo fractional order derivative of order α is given by

$${}_0^C\mathrm{D}_t^{\alpha}\mathrm{u}(t) = \frac{1}{\Gamma(n - \alpha)} \int_0^t \frac{\mathrm{u}^{(n)}(t)}{(t - \eta)^{\alpha + 1 - n}} d\eta, \; n - 1 < \alpha \leqslant n, n \in N, \tag{6}$$

provided that the right side is point wise defined on $(0, \infty)$, where $n = [\alpha] + 1$.

Lemma 2.3. *The solution of homogenous FODE*

$${}_0^C\mathrm{D}_t^{\alpha}\mathrm{u}(t) = 0 \tag{7}$$

is given by [9,12]

$$\mathrm{u}(t) = d_0 + d_1 t + d_2 t^2 + \ldots + d_{n-1} t^{n-1}, \tag{8}$$

such that $d_j \in \mathrm{R},\ j = 0, 1, 2, 3, \ldots, n-1$. The solutions of non-homogenous FODE

$$ {}_0^C\mathrm{D}_t^\alpha \mathrm{u}(t) = \mathrm{f}(t) \tag{9}$$

is given by

$$\mathrm{u}(t) = {}_0\mathrm{I}_t^\alpha \mathrm{f}(t) + d_0 + d_1 t + d_2 t^2 + \ldots + d_{n-1} t^{n-1}, \tag{10}$$

for some $d_j \in \mathrm{R},\ j = 0, 1, 2, \ldots, n-1$.

Lemma 2.4. *For $\alpha > 0$, the given result* [9,12]

$$ {}_0\mathrm{I}_t^\alpha [{}_0^C\mathrm{D}_t^\alpha u(t)] = \mathrm{u}(t) + d_0 + d_1 t + d_2 t^2 + \ldots + d_{n-1} t^{n-1}, \tag{11}$$

where $d_j \in \mathrm{R},\ \ j = 0, 1, 2, \ldots, n-1$ holds.

Also it follows that

$$ {}_0^C\mathrm{D}_t^\alpha t^k = \frac{\Gamma(1+k)}{\Gamma(1+k-\alpha)} t^{k-\alpha},\ {}_0\mathrm{I}_t^\alpha t^k = \frac{\Gamma(1+k)}{\Gamma(1+k+\alpha)} t^{k+\alpha},\ \text{for } k > -1,$$
$$\text{and } {}_0^C\mathrm{D}^\alpha\ [\mathrm{C}] = 0,\ \text{where C is a constant.} \tag{12}$$

Definition 2.5. The Mittag–Leffler function of one parameter is defined as [1]

$$E_\alpha(t) = \sum_{k=0}^{\infty} \frac{t^k}{\Gamma(k\alpha + 1)},\ \text{for } t \in \mathbb{C}, \alpha > 0. \tag{13}$$

Some of the recent work about fractional derivative can be found in the references [57–62].

2.2. *Introduction to Haar wavelet*

The scaling function for the family of HW on interval $[0, 1)$ is given by [63]:

$$h_1(s) = \begin{cases} 1 & \text{for} \quad s \in [0, 1), \\ 0 & \text{otherwise.} \end{cases} \tag{14}$$

The mother wavelets for the family of HWs defined on $[\zeta_1, \zeta_2)$ is given by

$$h_2(s) = \begin{cases} 1 & \text{for} \quad s \in [\zeta_1, \frac{\zeta_1+\zeta_2}{2}), \\ -1 & \text{for} \quad s \in [\frac{\zeta_1+\zeta_2}{2}, \zeta_2), \\ 0 & \text{otherwise.} \end{cases} \tag{15}$$

The other functions in the HW family HWF on subintervals of $[\zeta_1, \zeta_2)$ can be generated by the dilation and translation. Each function in the HWF on $[\zeta_1, \zeta_2)$ can be represented by

$$h_i(s) = \begin{cases} 1 & \text{for} \quad s \in [\xi_1, \xi_2), \\ -1 & \text{for} \quad s \in [\xi_2, \xi_3), \\ 0 & \text{otherwise} \qquad i = 1, 2, 3, \cdots, 2M, \quad N = 2M, \end{cases} \tag{16}$$

where

$$\xi_1 = \zeta_1 + (\zeta_2 - \zeta_1)\frac{d}{\varpi}, \tag{17}$$

$$\xi_2 = \zeta_1 + (\zeta_2 - \zeta_1)\frac{d + 0.5}{\varpi} \tag{18}$$

$$\text{and} \quad \xi_3 = \zeta_1 + (\zeta_2 - \zeta_1)\frac{d + 1}{\varpi}, \tag{19}$$

where the integer $\varpi = 2^r, r = 0, 1, 2, 3, \ldots, V;\ \ V = 2^M$, where M is a positive integer and the integer $d = 0, 1, 2, 3, \ldots \varpi - 1$.

HW is a piecewise constant function attaining three values $0, 1$ and -1. Any function belonging to $L_2[0, 1)$, the space of square integrable functions, can be approximated utilizing HW functions. Haar functions form an orthonormal bases for $L_2[0, 1)$. Any function $u(x)$ belonging to $L_2[0, 1)$ can be expressed as Haar series as: $u(x) = \sum_{i=1}^{\infty} \lambda_i h_i(s)$, where h_i are Haar functions [63]. For the approximation purpose, this series is truncated at finite terms.

Here we denote

$$p_{i,1}(s) = \int_0^s h_i(s) ds, \tag{20}$$

where $h_i(s)$ are defined in Eq. (16), now we have

$$p_{i,n+1}(s) = \int_0^s p_{i,n}(s) ds, \qquad n = 1, 2, \cdots \tag{21}$$

the value of $p_{i,1}(s)$ is

$$p_{i,1}(s) = \begin{cases} s - \xi_1 & \text{for} \quad s \in [\xi_1, \xi_2), \\ \xi_3 - s & \text{for} \quad s \in [\xi_2, \xi_3), \\ 0 & \text{otherwise.} \end{cases} \tag{22}$$

In general these integrals can be calculated utilizing Eq. (16),

$$p_{i,n}(s) = \begin{cases} 0 & \text{for} \quad s \in (0, 1], \\ \frac{1}{n!}(s - \xi_1)^n & \text{for} \quad s \in [\xi_1, \xi_2), \\ \frac{1}{n!}[(s - \xi_1)^n - 2(s - \xi_2)^n] & \text{for} \quad s \in [\xi_2, \xi_3), \\ \frac{1}{n!}[(s - \xi_1)^{-}2(s - \xi_2)^n + (s - \xi_3)^n] & \text{for} \quad s \in [\xi_3, 1), \qquad n = 1, 2, \cdots \end{cases} \tag{23}$$

Let $I = [\xi_1, \xi_2]$ be an interval on which the given FODE is to be solved, then the interval$I$ is divided into subintervals by using the following formula

$$t_k = \xi_1 + (\xi_2 - \xi_1)\frac{k - 0.5}{N}, \qquad k = 1, 2, 3, \cdots, N, \tag{24}$$

The points t_k are known as Collocation Point(CP) or nodal points. By applying the HW collocation technique to linear equation, we obtain a system of linear algebraic equations by substituting collocation points. The Gauss elimination technique is used to find the Haar coefficients. While applying the Haar wavelet collocation technique to nonlinear equation, we obtain a system of nonlinear algebraic equations by substituting collocation points. Broyden"s technique is used to find the Haar coefficients. At the end, by using these coefficients the numerical solution at the collocation points is obtained.

3. Numerical method

In this section, the HWCM is used for the solution of nonlinear and linear system of fractional differential Eqs. (1) and (3). The ordinary derivative is approximated by Haar functions and fractional derivatives are defined in the Caputo sense.

3.1. Linear case

Let $x'(t)$ and $y'(t)$ are in $L^2[0,1)$, then $x'(t)$ and $y'(t)$ can be written in Haar series as

$$x'(t)=\sum_{i=1}^{N}\lambda_i h_i(t),\qquad y'(t)=\sum_{i=1}^{N}\xi_i h_i(t), \tag{25}$$

where N is the number of CPs, $h_i(t)$ are the Haar functions and $\lambda_i,\ \xi_i$ are the unknown constant coefficients of Haar wavelets. Now integrating the above Eq. (33) from 0 to t we have

$$x(t)=x_0+\sum_{i=1}^{N}\lambda_i p_{i,1}(t)dt,\qquad y(t)=y_0+\sum_{i=1}^{N}\xi_i p_{i,1}(t)dt. \tag{26}$$

By applying the Caputo derivative to Eq. (1), and putting the values of $x(t)$ and $y(t)$, we have

$$\begin{aligned}\frac{1}{\Gamma(1-\alpha)}\int_0^t\frac{\sum_{i=1}^{N}\lambda_i h_i(\mu)d\mu}{(t-\mu)^{\alpha}}&=a\left(x_0+\sum_{i=1}^{N}\lambda_i p_{i,1}(t)\right)+b\left(y_0+\sum_{i=1}^{N}\xi_i p_{i,1}(t)\right)\\ \frac{1}{\Gamma(1-\beta)}\int_0^t\frac{\sum_{i=1}^{N}\xi_i h_i(\mu)d\mu}{(t-\mu)^{\beta}}&=c\left(x_0+\sum_{i=1}^{N}\lambda_i p_{i,1}(t)\right)+d\left(y_0+\sum_{i=1}^{N}\xi_i p_{i,1}(t)\right).\end{aligned} \tag{27}$$

Shifting known term to the right and unknown to the left, we have

$$\begin{aligned}&\frac{1}{\Gamma(1-\alpha)}\int_0^t\frac{\sum_{i=1}^{N}\lambda_i h_i(\mu)d\mu}{(t-\mu)^{\alpha}}-a\sum_{i=1}^{N}\lambda_i p_{i,1}(t)-b\sum_{i=1}^{N}\xi_i p_{i,1}(t)=ax_0+by_0\\ &\frac{1}{\Gamma(1-\beta)}\int_0^t\frac{\sum_{i=1}^{N}\xi_i h_i(\mu)d\mu}{(t-\mu)^{\beta}}-c\sum_{i=1}^{N}\lambda_i p_{i,1}(t)-\sum_{i=1}^{N}\xi_i p_{i,1}(t)=cx_0+dy_0.\end{aligned} \tag{28}$$

After simplification, we have

$$\begin{aligned}&\sum_{i=1}^{N}\lambda_i\left(\frac{1}{\Gamma(1-\alpha)}\int_0^t\frac{h_i(\mu)d\mu}{(t-\mu)^{\alpha}}-ap_{i,1}(t)\right)-b\sum_{i=1}^{N}\xi_i p_{i,1}(t)=ax_0+by_0\\ &-\sum_{i=1}^{N}\lambda_i c p_{i,1}(t)+\sum_{i=1}^{N}\xi_i\left(\frac{1}{\Gamma(1-\beta)}\int_0^t\frac{h_i(\mu)d\mu}{(t-\mu)^{\beta}}-p_{i,1}(t)\right)=cx_0+dy_0.\end{aligned} \tag{29}$$

Putting the CPs $t_j,\quad j=1,2,3,\ldots,2N$ we obtain

$$\begin{aligned}&\sum_{i=1}^{N}\lambda_i\left(\frac{1}{\Gamma(1-\alpha)}\int_0^{t_j}\frac{h_i(\mu)d\mu}{(t_j-\mu)^{\alpha}}-ap_{i,1}(t_j)\right)-b\sum_{i=1}^{N}\xi_i p_{i,1}(t_j)=ax_0+by_0\\ &-\sum_{i=1}^{N}\lambda_i c p_{i,1}(t_j)+\sum_{i=1}^{N}\xi_i\left(\frac{1}{\Gamma(1-\beta)}\int_0^{t_j}\frac{h_i(\mu)d\mu}{(t_j-\mu)^{\beta}}-p_{i,1}(t_j)\right)=cx_0+dy_0.\end{aligned} \tag{30}$$

The above integrals are calculated by following Haar integral formula:

$$\int_{a_1}^{a_2}f(s)ds\approx\frac{a_2-a_1}{N}\sum_{m=1}^{N}f(s_m)=\sum_{m=1}^{N}f\left(a_1+(a_2-a_1)\left(\frac{m-0.5}{N}\right)\right). \tag{31}$$

$$\begin{aligned}&\sum_{i=1}^{N}\lambda_i\left(\frac{t_j}{N\Gamma(1-\alpha)}\sum_{m=1}^{N}\frac{h_i(\mu_m)}{(t_j-\mu_m)^{\alpha}}-ap_{i,1}(t_j)\right)-b\sum_{i=1}^{N}\xi_i p_{i,1}(t_j)=ax_0+by_0\\ &-\sum_{i=1}^{N}\lambda_i c p_{i,1}(t_j)+\sum_{i=1}^{N}\xi_i\left(\frac{t_j}{N\Gamma(1-\beta)}\sum_{m=1}^{N}\frac{h_i(\mu_m)}{(t_j-\mu_m)^{\beta}}-p_{i,1}(t_j)\right)=cx_0+dy_0.\end{aligned} \tag{32}$$

The above system is solved by using Gauss elimination technique, to obtain the values of unknown Haar coefficients. The unknowns λ_i and ξ_i, for $i=1,2,3,\ldots,N$. The required solutions at CP is obtained by putting λ_i and ξ_i in Eq. (34).

3.2. Nonlinear case

Let $x'(t)$ and $y'(t)$ are in $L^2[0,1]$, then $x'(t)$ and $y'(t)$ can be written in the form of Haar series as

$$\begin{aligned}&x'(t)=\sum_{i=1}^{N}\lambda_i h_i(t),\quad y'(t)=\sum_{i=1}^{N}\xi_i h_i(t),\\ &z'(t)=\sum_{i=1}^{N}\zeta_i h_i(t).\end{aligned} \tag{33}$$

Now integrating above Eq. (33) from 0 to t we have

$$\begin{aligned}&x(t)=x_0+\sum_{i=1}^{N}\lambda_i p_{i,1}(t)dt,\quad y(t)=y_0+\sum_{i=1}^{N}\xi_i p_{i,1}(t)dt,\\ &z(t)=z_0+\sum_{i=1}^{N}\zeta_i p_{i,1}(t)dt.\end{aligned} \tag{34}$$

By putting the values of $x(t),y(t),z(t)$ and applying the Caputo derivative to Eq. (3), we have

$$\begin{aligned}\frac{1}{\Gamma(1-\alpha)}\int_0^t\frac{\sum_{i=1}^{N}\lambda_i h_i(\mu)d\mu}{(t-\mu)^{\alpha}}&=a\left(x_0+\sum_{i=1}^{N}\lambda_i p_{i,1}(t)\right)\\ \frac{1}{\Gamma(1-\beta)}\int_0^t\frac{\sum_{i=1}^{N}\xi_i h_i(\mu)d\mu}{(t-\mu)^{\beta}}&=b\left(x_0+\sum_{i=1}^{N}\lambda_i p_{i,1}(t)\right)^2\\ \frac{1}{\Gamma(1-\gamma)}\int_0^t\frac{\sum_{i=1}^{N}\zeta_i h_i(\mu)d\mu}{(t-\mu)^{\gamma}}&=c\left(x_0+\sum_{i=1}^{N}\lambda_i p_{i,1}(t)\right)\left(y_0+\sum_{i=1}^{N}\xi_i p_{i,1}(t)\right).\end{aligned} \tag{35}$$

After simplification, we get

$$\begin{aligned}&\frac{1}{\Gamma(1-\alpha)}\int_0^t\frac{\sum_{i=1}^{N}\lambda_i h_i(\mu)d\mu}{(t-\mu)^{\alpha}}-a\left(x_0+\sum_{i=1}^{N}\lambda_i p_{i,1}(t)\right)=0\\ &\frac{1}{\Gamma(1-\beta)}\int_0^t\frac{\sum_{i=1}^{N}\xi_i h_i(\mu)d\mu}{(t-\mu)^{\beta}}-b\left(x_0+\sum_{i=1}^{N}\lambda_i p_{i,1}(t)\right)^2=0\\ &\frac{1}{\Gamma(1-\gamma)}\int_0^t\frac{\sum_{i=1}^{N}\zeta_i h_i(\mu)d\mu}{(t-\mu)^{\gamma}}-c\left(x_0+\sum_{i=1}^{N}\lambda_i p_{i,1}(t)\right)\left(y_0+\sum_{i=1}^{N}\xi_i p_{i,1}(t)\right)=0.\end{aligned} \tag{36}$$

The above integrals are calculated by following formula:

$$\int_{a_1}^{a_2} f(s)ds \approx \frac{a_2 - a_1}{N}\sum_{m=1}^{N} f(s_m) = \sum_{m=1}^{N} f\left(a_1 + (a_2 - a_1)\left(\frac{m-0.5}{N}\right)\right). \quad (37)$$

$$\frac{t}{N\Gamma(1-\alpha)}\frac{\sum_{i=1}^{N}\lambda_i\sum_{m=1}^{N}h_i(\mu_m)}{(t-\mu_m)^{\alpha}} - \mathrm{a}\left(\mathrm{x}_0 + \sum_{i=1}^{N}\lambda_i p_{i,1}(t)\right) = 0$$
$$\frac{t}{N\Gamma(1-\beta)}\frac{\sum_{i=1}^{N}\xi_i\sum_{m=1}^{N}h_i(\mu_m)}{(t-\mu_m)^{\beta}} - \mathrm{b}\left(\mathrm{x}_0 + \sum_{i=1}^{N}\lambda_i p_{i,1}(t)\right)^2 = 0$$
$$\frac{t}{N\Gamma(1-\gamma)}\frac{\sum_{i=1}^{N}\zeta_i\sum_{m=1}^{N}h_i(\mu_m)}{(t-\mu_m)^{\gamma}} - \mathrm{c}\left(\mathrm{x}_0 + \sum_{i=1}^{N}\lambda_i p_{i,1}(t)\right)\left(\mathrm{y}_0 + \sum_{i=1}^{N}\xi_i p_{i,1}(t)\right) = 0. \quad (38)$$

Discretizing and substituting the nodal points, we obtain

$$F_j(\lambda_1,\ldots,\lambda_N,\xi_1,\ldots,\xi_N,\zeta_1,\ldots,\zeta_N) = \begin{cases} \frac{t_j}{N\Gamma(1-\alpha)}\frac{\sum_{i=1}^{N}\lambda_i\sum_{m=1}^{N}h_i(\mu_m)}{(t_j-\mu_m)^{\alpha}} - \mathrm{a}\left(\mathrm{x}_0 + \sum_{i=1}^{N}\lambda_i p_{i,1}(t_j)\right) \\ \frac{t_j}{N\Gamma(1-\beta)}\frac{\sum_{i=1}^{N}\xi_i\sum_{m=1}^{N}h_i(\mu_m)}{(t_j-\mu_m)^{\beta}} - \mathrm{b}\left(\mathrm{x}_0 + \sum_{i=1}^{N}\lambda_i p_{i,1}(t_j)\right)^2 \\ \frac{t_j}{N\Gamma(1-\gamma)}\frac{\sum_{i=1}^{N}\zeta_i\sum_{m=1}^{N}h_i(\mu_m)}{(t_j-\mu_m)^{\gamma}} - \mathrm{c}\left(\mathrm{x}_0 + \sum_{i=1}^{N}\lambda_i p_{i,1}(t_j)\right)\times \\ \left(\mathrm{y}_0 + \sum_{i=1}^{N}\xi_i p_{i,1}(t_j)\right). \end{cases} \quad (39)$$

This nonlinear system is solved by Broyden's technique. Solving this system we obtain the unknown Haar coefficients and finally the approximate solution at CPs can be obtained by utilizing these coefficients. The Jacobian of the above system is:

$$J = \begin{cases} \frac{\partial F_j}{\partial \lambda_m} = \frac{t_j}{N\Gamma(1-\alpha)}\sum_{m=1}^{N} h_i(\mu_m)(t_j-\mu_m)^{\alpha} - \mathrm{a}p_{m,1}(t_j), \quad \frac{\partial F_j}{\partial \xi_m} = 0 \\ \frac{\partial F_j}{\partial \zeta_m} = 0 \quad \frac{\partial F_j}{\partial \lambda_m} = -2\mathrm{b}\left(\mathrm{x}_0 + \sum_{i=1}^{N}\lambda_i p_{m,1}(t_j)\right) \\ \frac{\partial F_j}{\partial \xi_m} = \frac{t_j}{N\Gamma(1-\beta)} h_i(\mu_m)(t_j-\mu_m)^{\beta}, \\ \frac{\partial F_j}{\partial \zeta_m} = 0, \quad \frac{\partial F_j}{\partial \lambda_m} = \mathrm{y}_0 p_{m,1}(t_j)\sum_{i=1}^{N}\xi_i p_{,1}(t_j), \\ \frac{\partial F_j}{\partial \xi_m} = \mathrm{x}_0 p_{m,1}(t_j)\sum_{i=1}^{N}\lambda_i p_{m,1}(t_j), \quad \frac{\partial F_j}{\partial \zeta_m} = \frac{t_j}{N\Gamma(1-\zeta)} h_i(\mu_m)(t_j-\mu_m)^{\zeta}. \end{cases} \quad (40)$$

4. Numerical experiments

In this section, some test problems are provided to check the accuracy and efficiency of the proposed HWC technique. We have also computed the experimental rate of convergence $R_c(N)$ which is defined as [64]

$$R_c(N) = \frac{\log[\text{Maximum absolute errors}(N/2)/\text{Maximum absolute errors}(N)]}{\log 2}. \quad (41)$$

Example 4.1. Consider a coupled system of linear FODEs

$$\begin{cases} {}_0^C\mathrm{D}_t^{\alpha}\mathrm{x}(t) = \mathrm{x}(t) + \mathrm{y}(t), \ 0 < \alpha \leqslant 1, \\ {}_0^C\mathrm{D}_t^{\beta}\mathrm{y}(t) = -\mathrm{x}(t) + \mathrm{y}(t), \ 0 < \beta \leqslant 1, \end{cases} \quad (42)$$

with the initial conditions $\mathrm{x}(0) = 0, \mathrm{y}(0) = 1$. The exact solutions at integer values for $\alpha = \beta = 1$ are given by

$$\mathrm{x}(t) = e^t \sin t, \quad \mathrm{y}(t) = e^t \cos t, \quad \text{where} \quad t \in [0,\ 1]. \quad (43)$$

For this Test Problem 4.1, computing numerical solution via HWCM for distinct values of scale level N and compute the absolute error against the exact solutions at integer order. The corresponding maximum absolute errors $L_\infty = \|\text{Exact solution} - \text{Approximate solution}\|_\infty$ for the solution $x,\ y$ are provided in the given Table 1. The experimental rates of convergence for different number of collocation point is calculated which is approximately equal to 2 confirms the theoretical result proved by Majak et al. [64].

Also in Fig. 1, we provide the comparison between exact and numerical solutions which reveal that the method works as a powerful tool to find approximate solutions to various classes of FODEs. Further, the approximate solution at different fractional orders $\alpha,\ \beta$ are given in Fig. 2.

Example 4.2. Consider a system of nonlinear FODEs

$$\begin{aligned} &{}_0^C\mathrm{D}_t^{\alpha}\mathrm{x}(t) = \tfrac{3}{4}\mathrm{y}^2(t), \qquad 0 < \alpha \leqslant 1, \\ &{}_0^C\mathrm{D}_t^{\beta}\mathrm{y}(t) = \mathrm{x}(t)\mathrm{y}(t) - \tfrac{1}{8}\mathrm{y}^4(t) + 2, \qquad 0 < \beta \leqslant 1, \end{aligned} \quad (44)$$

with $\mathrm{x}(0) = 0,\ \mathrm{y}(0) = 0$. The exact solutions at fractional orders α, β are given by

$$\mathrm{x}(t) = \frac{6t^3}{\Gamma(5-\alpha)}, \qquad \mathrm{y}(t) = \frac{2t^{2-\beta}}{\Gamma(2-\beta)}, \text{where} \qquad t \in [0, 1]. \quad (45)$$

Upon HWCM computing numerical solution, we see that the absolute errors at different scale levels are much smallers which demonstrates the efficiency and usability of the considered technique. The maximum absolute errors at different scales level are given in Table 2. Further the comparison between exact and numerical solutions is provided in the adjacent Fig. 4.

Further in Fig. 3, we have provided plots at different fractional order corresponding to Test Problem 4.2.

Example 4.3. Consider a system of nonlinear FODEs as

$$\begin{aligned} &{}_0^C\mathrm{D}_t^{\alpha}\mathrm{x}(t) = -1002\mathrm{x}(t) + 1000\mathrm{y}^2(t), \qquad 0 < \alpha \leqslant 1, \\ &{}_0^C\mathrm{D}_t^{\alpha}\mathrm{y}(t) = \mathrm{x}(t) - \mathrm{y}(t) - \mathrm{y}^2(t), \qquad 0 < t \leqslant 2, \end{aligned} \quad (46)$$

with $\mathrm{x}(0) = 1,\ \mathrm{y}(0) = 1$. The exact solutions at fractional orders $\alpha,\ \beta$ are given by

$$\mathrm{x}(t) = E_\alpha(-2t), \qquad \mathrm{y}(t) = E_\beta(-t), \text{where} \qquad t \in [0, 1] \quad (47)$$

Table 1 Maximum absolute errors for Test Problem 4.1 corresponding to different scale values.

I	$N = 2^{I+1}$	Maximum absolute errors for x	R_c	Maximum absolute errors for y	R_c
1	4	2.53584×10^{-2}	—	5.98245×10^{-2}	—
2	8	6.54778×10^{-3}	1.9534	1.67653×10^{-2}	1.8353
3	16	1.65046×10^{-3}	1.9881	4.43142×10^{-3}	1.9196
4	32	4.13150×10^{-4}	1.9981	1.13860×10^{-3}	1.9605
5	64	1.03367×10^{-4}	1.9989	2.88535×10^{-4}	1.9804
6	128	2.58462×10^{-5}	1.9998	7.26216×10^{-5}	1.9903
7	256	6.46179×10^{-6}	1.9999	1.82165×10^{-5}	1.9952
8	512	1.61546×10^{-6}	2.0000	4.56177×10^{-6}	1.9976
9	1024	4.03865×10^{-7}	2.0000	1.14139×10^{-6}	1.9988

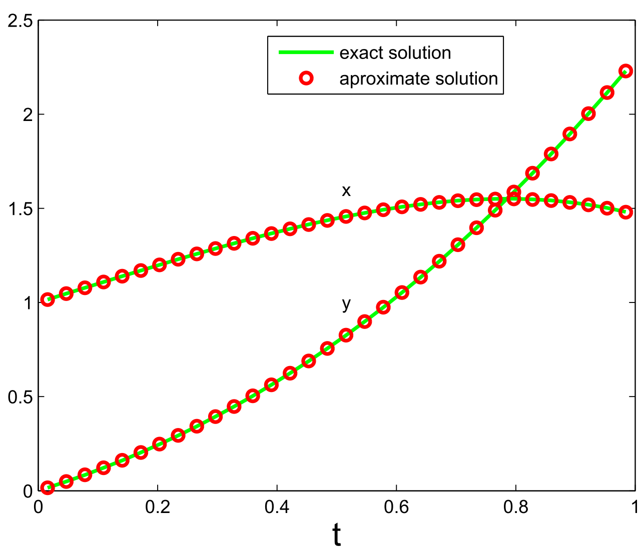

Fig. 1 Comparison of both (approximate and exact) solution for 32 nodal points for Test Problem 4.1.

and E is Mittag–Leffler function.

Again by using HWCM to compute numerical solution, we see that the absolute errors at different scale levels are much smallers which demonstrates the efficiency and usability of the considered techniques. The maximum absolute errors at different scales level are given in Table 3.

Further the comparison between exact and numerical solutions is provided in the adjacent Fig. 5.

The approximate solutions at different fractional orders are given in Fig. 6.

Example 4.4. Consider the following nonlinear system of FODEs:

$$\begin{aligned} &{}_0^C\mathrm{D}_t^\alpha \mathrm{x}(t) = \mathrm{x}(t), \qquad 0 < \alpha \leqslant 1,\\ &{}_0^C\mathrm{D}_t^\beta \mathrm{y}(t) = 2\mathrm{x}^2(t), \qquad 0 < \beta \leqslant 1,\\ &{}_0^C\mathrm{D}_t^\gamma \mathrm{z}(t) = 3\mathrm{x}(t)\mathrm{y}(t), \qquad 0 < \gamma \leqslant 1, \end{aligned} \tag{48}$$

with the initial conditions $\mathrm{x}(0) = 1$, $\mathrm{y}(0) = 1$, $\mathrm{z}(0) = 1$. The exact solutions at fractional orders α, β, γ are given by

$$\begin{aligned} &\mathrm{x}(t) = E_\alpha(t), \qquad \mathrm{y}(t) = E_\beta(2t)\\ &\mathrm{z}(t) = E_\gamma(3t), \text{ where } \quad t \in [0, 1], \end{aligned} \tag{49}$$

where E is known as Mittag–Leffler function.

With the help HWCM we compute numerical results for the coupled system of nonlinear FODEs, we see that the proposed method can be used as a powerful tools to find numerical solutions to the aforesaid equations. Further we compute maximum absolute errors at different scale levels in the given Table 4.

Also the comparison between exact and numerical solution by using HWCM, we provide in Fig. 7. From this figure it is obvious that exact and numerical solutions have close agreement which show the accuracy of the proposed method.

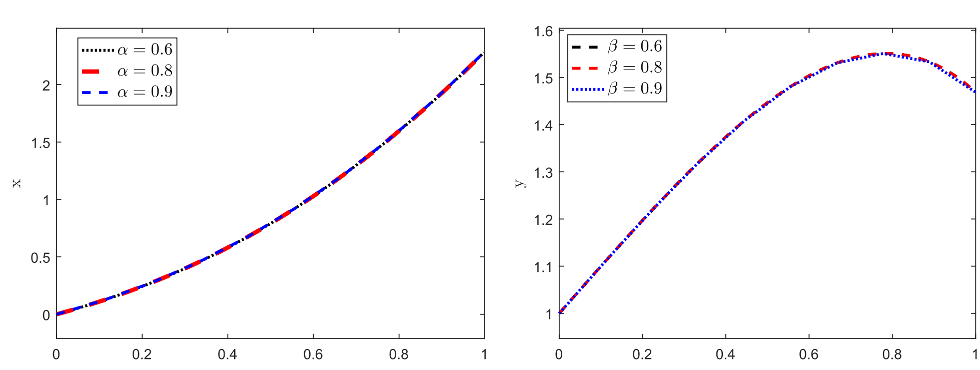

Fig. 2 Approximate solutions for different values of α and β, for Test Problem 4.1 corresponding to $N = 20$.

Table 2 Maximum absolute errors for Test Problem 4.2 corresponding to different scale values.

I	$N = 2^{I+1}$	Maximum absolute errors for x	R_c	Maximum absolute errors for y	R_c
1	4	3.43132×10^{-2}	—	1.24768×10^{-2}	—
2	8	9.43685×10^{-3}	1.8624	3.58431×10^{-3}	1.7995
3	16	2.48763×10^{-3}	1.9235	9.60782×10^{-4}	1.8994
4	32	6.37703×10^{-4}	1.9638	2.49109×10^{-4}	1.9474
5	64	1.59498×10^{-4}	1.9993	6.39858×10^{-5}	1.9610
6	128	3.78216×10^{-5}	2.0763	1.68077×10^{-5}	1.9286
7	256	7.10139×10^{-6}	2.4130	4.90903×10^{-6}	1.9756

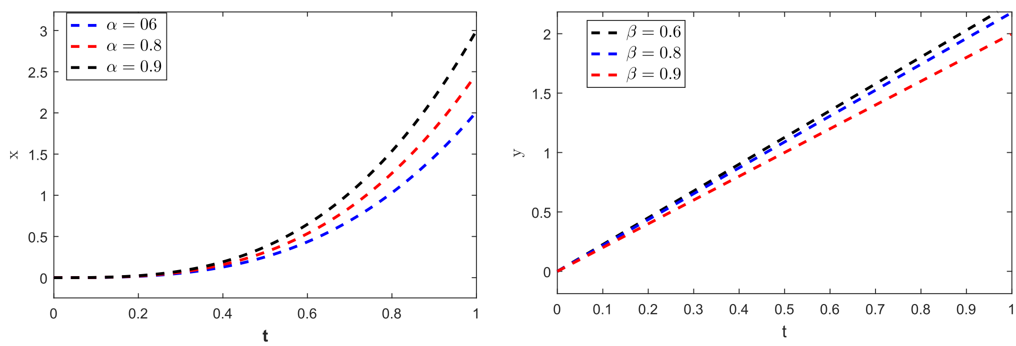

Fig. 3 Approximate solutions for different values of α and β, for Test Problem 4.2 corresponding to $N = 20$.

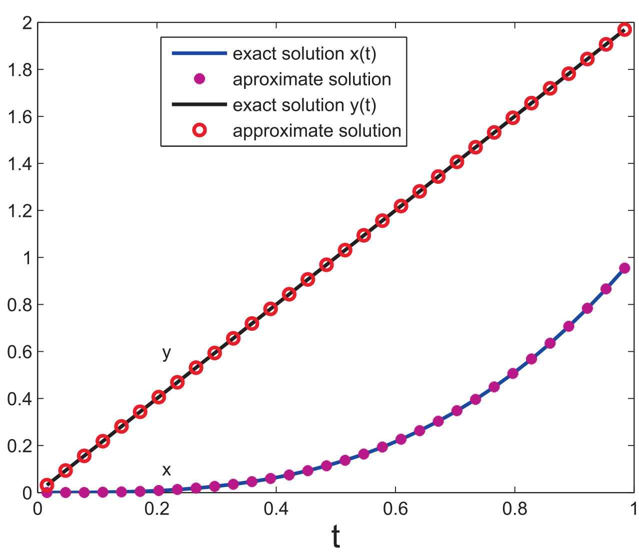

Fig. 4 Comparison of both (approximate and exact) solution for 32 mesh points for Test Problem 4.2.

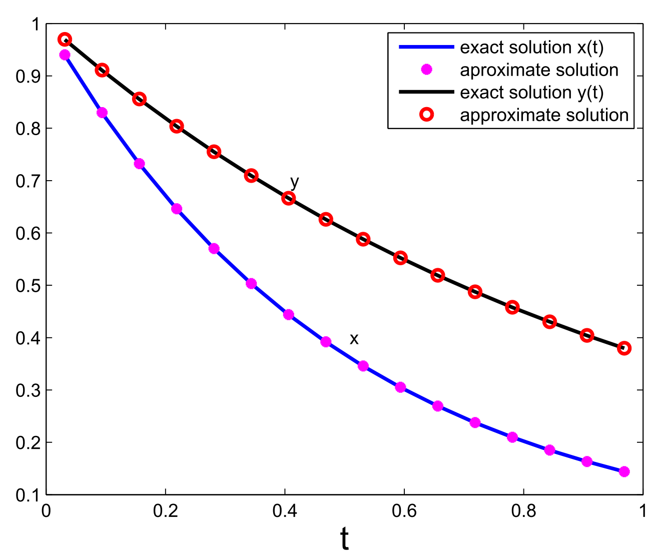

Fig. 5 Comparison of both (approximate and exact) solution for 16 nodal points for Test Problem 4.3.

Table 3 Maximum absolute errors for Test Problem 4.3 corresponding to different scale values.

I	$N = 2^{I+1}$	Maximum absolute errors for x	R_c	Maximum absolute errors for y	R_c
1	4	3.36789×10^{-2}	—	2.12309×10^{-2}	—
2	8	1.14395×10^{-2}	1.5578	6.40283×10^{-3}	1.7294
3	16	3.37653×10^{-3}	1.7604	1.76660×10^{-3}	1.8577
4	32	9.29181×10^{-4}	1.8615	4.64595×10^{-4}	1.9269
5	64	2.52180×10^{-4}	1.8815	1.06582×10^{-4}	2.1240
6	128	6.43774×10^{-5}	1.9698	3.06058×10^{-5}	1.8001
7	256	1.77412×10^{-5}	1.8595	5.37993×10^{-6}	2.5081
8	512	4.47875×10^{-6}	1.9859	1.37005×10^{-6}	1.9734

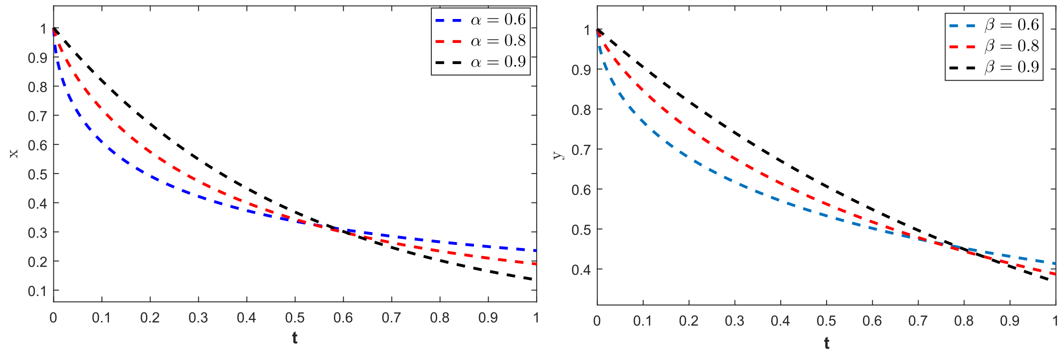

Fig. 6 Approximate solutions at $N = 20$ for Test Problem 4.3 against different fractional values of α, β.

Table 4 Maximum absolute errors for Test Problem 4.4 corresponding to different scale values.

I	$N = 2^{I+1}$	Maximum absolute errors for x	Maximum absolute errors for y	Maximum absolute errors for z
1	4	8.13468×10^{-3}	6.72459×10^{-2}	3.98281×10^{-1}
2	8	2.11925×10^{-3}	1.79610×10^{-2}	1.09190×10^{-1}
3	16	5.41185×10^{-4}	4.64604×10^{-3}	2.86363×10^{-2}
4	32	1.36762×10^{-4}	1.18179×10^{-3}	7.33582×10^{-3}
5	64	3.43767×10^{-5}	2.98037×10^{-4}	1.85667×10^{-3}
6	128	8.61762×10^{-6}	7.48362×10^{-5}	4.67044×10^{-4}
7	256	2.15735×10^{-6}	1.87501×10^{-5}	1.17123×10^{-4}

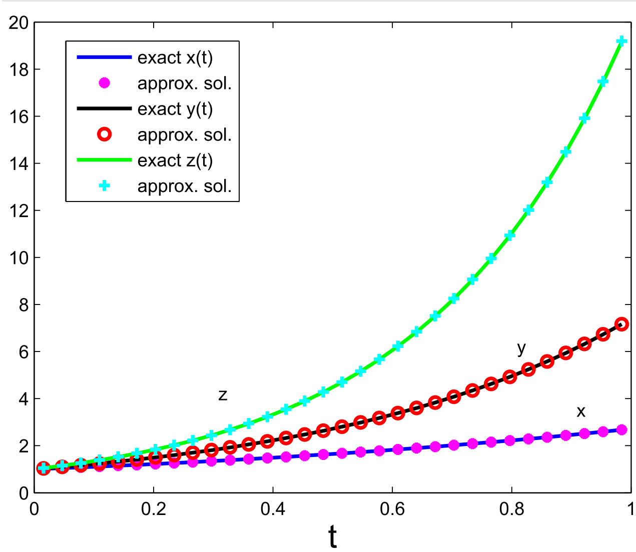

Fig. 7 Comparison of both (exact and approximate) solution for $N = 32$ for Test Problem 4.4 at $\alpha = \beta = \gamma = 1$.

Further enlarging the numbers of collocation points the absolute error may further be decreased which show the applicability of the considered method.

Further in Fig. 8 we have provided comparison between exact and numerical solutions.

5. Conclusion

In this paper we have successfully extended the HWCM for the solutions to linear and nonlinear FODEs under initial conditions. The mentioned method has been worked as a powerful and efficient techniques to establish numerical results for both linear and nonlinear FODEs. In future this method can be used to solve other problems which are highly nonlinear devoted to partial differential equations of fractional order. Also we have compared our results with the exact solutions of the considered test problems at integer order. We see from the tables and plots that the computed numerical results have close agreement with the corresponding exact solutions at integer order. The experimental rates of convergence for different

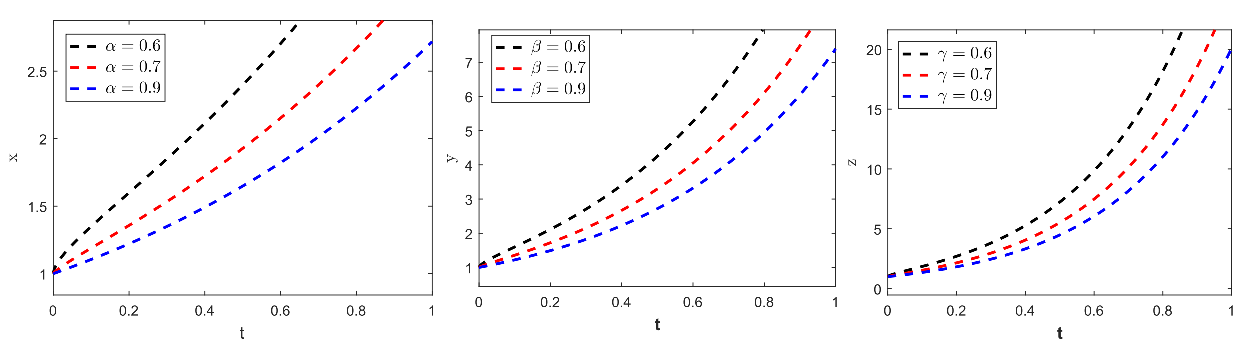

Fig. 8 Approximate solutions at $N = 20$ for Test Problem 4.4 against different fractional values of α, β, γ.

number of collocation point is also calculated, which is approximately equal to 2.

Declaration of Competing Interest

The authors declare that they have no known competing financial interests or personal relationships that could have appeared to influence the work reported in this paper.

Acknowledgment

The authors would like to express their sincere thanks to the referees for their careful review of this manuscript and their useful suggestions which led to the improved version. In addition, the authors would like to thank both Prince Sultan University (research group Nonlinear Analysis Methods in Applied Mathematics (NAMAM) group number RG-DES2017-01-17) and United Arab Emirates University (Grant No. 31S363-UPAR (4) 2018) for supporting this work.

References

[1] I. Podlubny, Fractional Differential Equations, Academic Press, San Diego CA, 1999.
[2] C.F. Lorenzo, T.T. Hartley, Variable order and distributed order fractional operators, Nonlinear Dyn. 29 (2002) 57–98.
[3] M. Caputo, Linear models of dissipation whose Q is almost frequency independent, Part II. Geophys. J. Int. 135 (1967) 529–539.
[4] A. Atangana, S.T.A. Badr, Extension of the RLC electrical circuit to fractional derivative without singular kernel, Adv. Mech. Eng. 7 (2015) 1–6.
[5] A.M. El-Sayed, S.Z. Rida, A.A.M. Arafa, Exact solutions of fractional-order biological population model, Commun. Theor. Phys. 52 (6) (2009) 992–996.
[6] A. Atangana, Numerical solution of space-time fractional order derivative of groundwater flow equation. In: International Conference of Algebra and Applied Analysis, Istanbul, June (20)2 (2012), pp. 20–24.
[7] R.A. Khan, M. Rehman, Existence of multiple positive solutions for a general system of fractional differential equations, Commun. Appl. Nonlin. Anal. 18 (2011) 25–35.
[8] G. Wu, D. Baleanu, Stability analysis of impulsive fractional difference equations, Fract. Calc. Appl. Anal. 21 (2018) 354–375.
[9] A. Anguraj, P. Karthikeyan, M. Rivero, J. Trujillo, On new existence results for fractional integro-differential equations with impulsive and integral conditions, Comput. Math. Appl. 66 (12) (2014) 2587–2594.
[10] Z. Han, H. Lu, C. Zhang, Positive solutions for eigenvalue problems of fractional differential equation with generalized p-Laplacian, Appl. Math. Comput. 257 (2015) 526–536.
[11] T. Ma, Y. Tian, Q. Huo, Y. Zhang, Boundary value problem for linear and nonlinear fractional differential equations, Appl. Math. Lett. 86 (2018) 1–7.
[12] K. Shah, H. Khalil, R.A. Khan, Investigation of positive solution to a coupled system of impulsive boundary value problems for nonlinear fractional order differential equations, Chaos, Solitons Fractals 77 (2015) 240–246.
[13] K. Shah, R.A. Khan, Iterative scheme for a coupled system of fractional-order differential equations with three-point boundary conditions, Mathe. Methods Appl. Sci. 41 (3) (2018) 1047–1053.
[14] A. Ali, B. Samet, K. Shah, R.A. Khan, Existence and stability of solution to a toppled systems of differential equations of non-integer order, Boundary Value Probl. 2017 (2017) 16.
[15] A. Ali, K. Shah, F. Jarad, V. Gupta, T. Abdeljawad, Existence and stability analysis to a coupled system of implicit type impulsive boundary value problems of fractional-order differential equations, Adv. Diff. Eq. 2019 (2019) 101.
[16] T. Abdeljawad, Q.M. Al-Mdallal, F. Jarad, Fractional logistic models in the frame of fractional operators generated by conformable derivatives, Chaos Solitons Fractals 119 (2019) 94–101.
[17] F. Jarad, T. Abdeljawad, Z. Hammouch, On a class of ordinary differential equations in the frame of Atangana-Baleanu fractional derivative, Chaos Solitons Fractals 117 (2018) 16–20.
[18] Y.Y. Gambo, R. Ameen, F. Jarad, T. Abdeljawad, Existence and uniqueness of solutions to fractional differential equations in the frame of generalized Caputo fractional derivatives, Adv. Diff. Eq. 2018 (2018) 134.
[19] R. Ameen, F. Jarad, T. Abdeljawad, Stability for delay fractional differential equations with a generalized Caputo derivative, Filomat 32 (15) (2018) 5265–5274.
[20] K. Shah, H. Khalil, R.A. Khan, Analytical solutions of fractional order diffusion equations by natural transform method, Iran J. Sci. Technol. (Trans Sci:A) 2016 (2016) 1–12.
[21] D. Kumar, J. Singh, Sushela, Application of homotopy analysis transform method to fractional biological population model, Romanian Reports Phys. 65 (1) (2013) 63–75.
[22] F. Haq, K. Shah, G. Rahman, M. Shahzad, Numerical solution of fractional order smoking model via Laplace Adomian decomposition method, Alexandria Eng. J. 57 (2) (2018) 1061–1069.
[23] Y. Li, K. Shah, R.A. Khan, Iterative technique for coupled integral boundary value problem of non-integer order differential equations, Adv. Diff. Eq. 2017 (2017) 251.
[24] A. Atangana, E. Alabraoye, Solving a system of fractional partial differential equations arising in the model of HIV infection of CD4+ cells and attractor one-dimensional Keller-Segel equations, Adv. Diff. Eq. 94 (2013) 1–14.
[25] A. Atangana, A. Secer, The time-fractional coupled-Korteweg-de-Vries equations, Abstr. Appl. Anal. (2013) 14.
[26] S. Maitama, A hybrid natural transform homotopy perturbation method for solving fractional partial differential equations, Int, J. Differ. Equ. 2016 (2016) 14.
[27] Q.M. Al-Mdallal, M.A. Hajji, A convergent algorithm for solving higher-order nonlinear fractional boundary value problems, Fract. Calculus Appl. Anal. 18 (6) (2015) 1423–1440.
[28] Q.M. Al-Mdallal, M.I. Syam, An efficient method for solving non-linear singularly perturbed two points boundary-value problems of fractional order, Commun. Nonlin. Sci. Numr. Simul. 17 (6) (2012) 2299–2308.
[29] Q.M. Al-Mdallal, K.A. Abro I. Khan, Analytical solutions of fractional Walter's B fluid with applications Complexity, 2018 (2018).
[30] Q.M. Al-Mdallal, A.S. Abu Omer, Fractional-order Legendre-collocation method for solving fractional initial value problems, Appl. Math. Comput. 321 (2018) 74–84.
[31] Q.M. Al-Mdallal, On fractional-Legendre spectral Galerkin method for fractional Sturm-Liouville problems, Chaos Solitons Fractals 116 (2018) 261–267.
[32] Q. Liu, An implicit RBF meshless approach for time fractional diffusion equations, Comput. Mech. 48 (1) (2011) 1–12.
[33] A. Saadatmandi, M. Dehghan, A tau approach for solution of the space fractional diffusion equation, Comput. Math. Appl. 62 (3) (2011) 1135–1142.
[34] D. Ziane, M.H. Cherif, Variational iteration transform method for fractional differential equations, J. Interdiscip. Math. 21 (1) (2018) 185–199.
[35] M. Rehman, R.A. Khan, The Legendre wavelet method for solving fractional differential equations, Commun. Nonlin. Sci. Numer. Simulat. 16 (2011) 4163–4173.

[36] Y. Li, K. Shah, Numerical solutions of coupled systems of fractional order partial differential equations, Adv. Mathe. Phys. 2017 (2017) 14.
[37] K. Shah, J. Wang, A numerical scheme based on nondiscretization of data for boundary value problems of fractional order differential equations, RACSAM 2018 (2018) 1–18.
[38] O.A. Arqub, Numerical algorithm for the Solutions of fractional order systems of Dirichlet function types with comparative analysis, Fundamenta Informaticae 166 (2) (2019) 111–137.
[39] O.A. Arqubr, N. Shawagfeh, Application of reproducing kernel algorithm for solving Dirichlet Time-fractional diffusion-Gordon types equations in porous media, J. Porous Media 22 (4) (2019) 411–434.
[40] O.A. Arqub, Application of residual power series method for the solution of time-fractional Schrödinger equations in one-dimensional space, Fundamenta Informaticae 166 (2) (2019) 87–110.
[41] O.A. Arqub, Numerical solutions of systems of first-order, two-point BVPs based on the reproducing kernel algorithm, Calcolo 55 (2018) 1–28.
[42] I. Horng, J. Chou, Shifted Chebyshev direct method for solving variational problems, I.J. Syst. Sci. 16 (1985) 855–861.
[43] A. Saadatmandi, M. Dehghan, M.R. Azizi, The Sine-Legendre collocation method for a class of fractional convection-diffusion equations with variable coefficients, Commun. Nonlinear Sci. Numer. Simul. 17 (11) (2012) 4125–4136.
[44] C. Chen, C. Hsiao, Haar wavelet method for solving lumped and distributed-parameter systems, IEE P.-Contr. Theor. Appl. 144 (1997) 87–94.
[45] M.H. Heydari, M.R. Hooshmandasl, F.M. Maalek Ghaini, M. Li, Chebyshev wavelets method for solution of nonlinear fractional integrodifferential equations in a large interval, Adv. Mathe. Phys. 2013 (2013) 12, Article ID 482083.
[46] A.A. Cardoso, F.H. Vieira, Adaptive estimation of Haar wavelet transform parameters applied to fuzzy prediction of network traffic, Signal Process. 151 (2018) 155–159.
[47] R. Reisenhofer, S. Bosse, G. Kutyniok, T. Wiegand, A Haar wavelet-based perceptual similarity index for image quality assessment, Signal Process.: Image Commun. 61 (2018) 33–43.
[48] B.J. Adiguna, A.G. Buchanb, A. Adama, S. Dargavillea, M.A. Goffina, C.C. Paina, A Haar wavelet method for angularly discretising the Boltzmann transport equation, Prog. Nucl. Energy 108 (2018) 295–309.
[49] U. Lepik, H. Lepik, Haar Wavelets with Applications, Springer, 2014.
[50] K. Kotharia, U. Mehtaa, J. Vanualailaib, A novel approach of fractional-order time delay system modeling based on Haar wavelet, ISA Trans. 80 (2018) 371–380.
[51] Q. Dai, Q. Cao, Y. Chen, Frequency analysis of rotating truncated conical shells using the Haar wavelet method, Appl. Math. Model. 57 (2018) 603–613.
[52] S.M. Aznam, M.S. Chowdhury, Generalized Haar wavelet operational matrix method for solving hyperbolic heat conduction in thin surface layers, Res. Phys. 11 (2018) 243–252.
[53] R. Singh, H. Garg, V. Guleria, Haar wavelet collocation method for Lane-Emden equations with Dirichlet, Neumann and Neumann-Robin boundary conditions, J. Comput. Appl. Math. 346 (2019) 150–161.
[54] Y. Li, W. Zhao, Haar wavelet operational matrix of fractional order integration and its applications in solving the fractional order differential equations, Appl. Math. Comput. 216 (2010) 2276–2285.
[55] M. Rehman, R.A. Khan, A numerical method for solving boundary value problems for fractional differential equations, Appl. Math. Model. 36 (3) (2012) 894–907.
[56] A. Neamaty, B. Agheli, R. Darzi, Solving fractional partial differential equation by using wavelet operational method, J. Math. Comput. Sci. 7 (2013) 230–240.
[57] A.A. Omar, Numerical algorithm for the Solutions of fractional order systems of Dirichlet function types with comparative analysis, Fundamenta Informaticae 166 (2) (2019) 111–137.
[58] A. Atangana, J.F.G. Aguilar, M.O. Kolade, J.Y. Hristo, Fractional differential and integral operators with non-singular and non-local kernel with application to nonlinear dynamical systems, Chaos, Solitons Fractals 132 (2019) 109493.
[59] H. Heydaria, A. Atangana, An optimization method based on the generalized Lucas polynomials for variable-order space-time fractional mobile-immobile advection-dispersion equation involving derivatives with non-singular kernels, Chaos, Solitons Fractals 132 (2020) 109588.
[60] H. Heydaria, A. Atangana, Solutions of the linear and nonlinear differential equations within the generalized fractional derivatives, Chaos: Interdiscip. J. Nonlinear Sci. 29 (2) (2019) 023108.
[61] A. Akgül, A novel method for a fractional derivative with non-local and non-singular kernel, Chaos, Solitons Fractals 114 (2018) 478–482.
[62] A. Atangana, A. Akgül, K.M. Owolabi, Analysis of fractal fractional differential equations, Alexandria Eng. J. 59 (2020) 1117–1134.
[63] I. Aziz, R. Amin, Numerical solution of a class of delay differential and delay partial differential equations via Haar wavelet, Appl. Math. Model. 40 (2016) 10286–10299.
[64] J. Majak, B. Shvartsman, K. Karjust, M. Mikola, A. Haavajoe, M. Pohlak, On the accuracy of the Haar wavelet discretization method, Comp. Part B 80 (2015) 321–327.